RAPORT NR INP-1441/PH

Quark Matter in a Chiral Chromodielectric Model

Wojciech Broniowski[a], Marko Cibej[b], Marek Kutschera[a]

and

Mitja Rosina[b†]

[a]H. Niewodniczański Institute of Nuclear Physics,
31-342 Kraków, Poland

[b] Institute Jožef Stefan, E. Kardelj University,
P.O. BOX 100, YU-61111 Ljubljana, Yugoslavia

March 1989

ABSTRACT

Zero and finite temperature quark matter is studied in a chiral chromodielectric model with quark, meson and chromodielectric degrees of freedom. Mean field approximation is used. Two cases are considered: two-flavor and three-flavor quark matter. It is found that at sufficiently low densities and temperatures the system is in a chirally broken phase, with quarks acquiring effective masses of the order of 100 MeV. At higher densities/temperatures a chiral phase transition occurs, and the quarks become massless. A comparison to traditional nuclear physics suggests that the chirally broken phase with massive quark gas may be the ground state of matter at densities of the order of a few nuclear saturation densities.

1. INTRODUCTION

Over the past few years various chromodielectric models have become popular[1-9]. These models are based on the old idea[10] that the phenomenon of confinement can be described by vanishing of the chromodielectric constant in the vacuum, $\varepsilon_{vac} = 0$. In chromodielectric models the dielectric constant ε is treated as a dynamical effective field. Several attempts have been made to justify these models, starting from QCD on the lattice[1,11-14]. The form of the effective lagrangians that follows from such considerations has, in general, the following structure:

$$\mathcal{L} = \bar{\psi}\, \partial_\mu \gamma^\mu\, \psi - \bar{\psi}\, M\, \psi\, /\chi^p + 1/2\ \chi_0^2 (\partial^\mu \chi)^2 - U(\chi) + \mathcal{L}' \quad , \qquad (1)$$

where ψ is the quark field, χ is the (dimensionless) chromodielectric field, p is some positive power, M is the quark mass, χ_0 is a scale of dimension of energy, $U(\chi)$ is the χ-field potential, and $\mathcal{L}'$ contains terms with color octet fields, and possibly other effective degrees of freedom. The chromodielectric constant is related to the chromodielectric field in the following manner[1]

$$\varepsilon = \chi^4 \quad , \qquad (2)$$

hence to ensure $\varepsilon_{vac} = 0$ one requires that $\chi_{vac} = 0$.

The key element of chromodielectric models is that the effective quark mass, M/χ^p, becomes infinite in the vacuum, which in the case of baryons forces the quarks to be confined in bag-like objects[2-8], very much like in the old MIT bag model.[15]

The difference is that in the case of chromodielectric models, the bag is generated selfconsistently through the interaction with the dynamical field χ.

Since QCD possesses an approximate chiral symmetry, any realistic effective theory of strong interactions has to respect this symmetry. Chiral extensions of chromodielectric models have been proposed and studied in the context of models of hadrons by several authors[4,5,8,9,14]. The modification in the lagrangian (1) amounts to the replacement of the mass term by a chirally invariant form involving σ and π mesons, and to adding a suitable σ-π interaction. The lagrangian of the chiral chromodielectric model which we are going to study in this paper has the form

$$\mathcal{L} = \bar{\psi}\, i\partial\!\!\!/\, \psi + g^p\, \bar{\psi}(\sigma + i\gamma_5 \vec{\tau}\cdot\vec{\pi})\psi\, /\chi^p + 1/2\, \chi_0^2(\partial^\mu \chi)^2 - W(\chi) + \\ + 1/2\, (\partial^\mu \sigma)^2 + 1/2\, (\partial^\mu \vec{\pi})^2 - U(\sigma,\vec{\pi}) \qquad (3)$$

The potential $U(\sigma,\vec{\pi})$ has the "Mexican Hat" shape[16], which leads to spontaneous chiral symmetry breaking, with $\sigma_{vac} = -F_\pi$, where $F_\pi = 93$ MeV is the pion decay constant. The coupling constant g is dimensionless. The effective mass of the quark in this model is

$$m_q^{eff} = - g^p \sigma/\chi^p \qquad (4)$$

In the vacuum, due to spontaneous chiral symmetry breaking, σ is nonzero, and since $\chi_{vac} = 0$, m_q^{eff} becomes infinite, as in the non-chiral model (1).

The main purpose of this work is to study the chiral phase transition generated by lagrangian (3). Our approach parallels the treatment of the fermion-meson system in the Walecka model[17]. Specifically, we use the mean field approximation, i.e. the effective meson and chromodielectric fields are treated as classical fields, and no quantum effects for the quarks are included. We find that at sufficiently low densities and temperatures, the system is in a chirally broken phase, with $\sigma \neq 0$, and with massive quarks (cf. eqn.(4)). As the matter is compressed, at some point a first order phase transition to a chirally symmetric phase occurs, and at higher densities the ground state of the system becomes just a gas of massless quarks, with $\sigma = 0$ (in this work we ignore the effects of current quark masses).

The paper is organized as follows: In Sect. II and III we study the zero temperature matter. Two cases are considered: isospin-symmetric quark matter (Sect. II), with equal amounts of up and down quarks, and charge-neutral quark matter (Sect. III), with equal amounts of up, down and strange quarks. The results of Sec. III may be applied to models of neutron stars. In Sect. IV we study the two-flavor quark matter at finite temperatures. This situation may be realized in relativistic heavy-ion collisions, as well as in the early universe.

II. TWO FLAVOR MATTER AT ZERO TEMPERATURE

For simplicity of calculation, we make the assumption that the system is uniform. Thus, the mean χ and σ fields have constant values throughout the whole space, and the pion field vanishes[17]. The valence quarks occupy plane wave states of positive energy, up to the fermi momentum k_F. The expression to minimize is the energy per baryon number,

$$E/N = \frac{\gamma \int d^3k/(2\pi)^3 \sqrt{(m_q^{eff})^2 + k^2}\ \theta(k_F - |\vec{k}|) + U(\sigma) + W(\chi)}{\gamma/3 \int d^3k/(2\pi)^3\ \theta(k_F - |\vec{k}|)} , \quad (6)$$

where $\gamma = 2\times2\times3$ is the spin-flavor-color degeneracy, m_q^{eff} is given in (4), k_F is the fermi momentum, and the σ and χ potentials are given by

$$U(\sigma) = \frac{m_\sigma^2}{8F_\pi^2} (\sigma^2 - F_\pi^2)^2 , \quad (7a)$$

$$W(\chi) = 1/2\ M_\chi^2\ \chi_0^2\ \chi^2 . \quad (7b)$$

Potential (7a) is the familiar "Mexican Hat"[16], with the pion field set to zero, and for the case of $m_\pi = 0$. The quantity m_σ is the mass of the σ meson. Potential (7b) consists just of a mass term for the chromodielectric field.

The model seemingly has five parameters: g, m_σ, M_χ, χ_0 and p. However, introducing a new variable $\chi' = M_\chi \chi_0\ \chi$, potential (7b) becomes just $U(\chi') = 1/2\ \chi'^2$, and the effective quark mass (4) takes the form $m_q^{eff} = -(gM_\chi\chi_0)^p\sigma/\chi'^p$. Thus, expression (6) depends effectively on three parameters: m_σ, $gM_\chi\chi_0$ and p. For

convenience we denote

$$G = \sqrt{g^2 \chi_0} \quad , \tag{8}$$

which is a free parameter of dimension of energy. Throughout this paper we use $m_\sigma = 1.2$ GeV[5]. The choice of power p is more subtle. Various authors have their preferred choices of this parameter, ranging from 1[4,5,6], through 3/2[14] to 2[18]. Here we do not want to make a judgement on which choice is better justified. We present results mostly for p = 2, however we will also show the qualitative conclusions do not depend on the specific choice of p.

To find the configuration with minimum energy per unit of baryon number, expression (6) is minimized with respect to χ' and m_q^{eff} at a fixed value of k_F. We use χ' and m_q^{*eff} as independent variables, rather than χ' and σ, to avoid divisions by 0 in eqn. (4). The field σ is thus replaced by $\sigma = -m_q^{*eff}(\chi'/G^2)^p$ in eqn. (7a). The results for p = 2 and G = 0.217 GeV are displayed in Fig. 1, where we plot the energy per baryon number (a), and the value of mean fields and m_q^{*eff} (b) versus the volume per baryon number.

At high densities the ground state is in the chirally restored phase (solid line, labeled $\sigma = 0$), for which both m_q^{*eff} and χ' vanish. In this case expression (6) has a particularly simple form

$$E/N_{chiral} = \frac{\gamma \int d^3k/(2\pi)^3 \; k \; \theta(k_F - |\vec{k}|) + B}{\gamma/3 \int d^3k/(2\pi)^3 \; \theta(k_F - |\vec{k}|)} \quad , \tag{9}$$

where $B = m_\sigma^2 F_\pi^2/8$ has the interpretation of the volume density of the energy of the chirally symmetric vacuum. It plays the same role in expression (9) as the bag constant of the MIT bag model[15,19]. In the limit of large densities, E/N_{chiral} behaves as k_F, which is a feature of a relativistic fermi gas. For low densities, E/N_{chiral} behaves as k_F^{-3}, and in fact the solid curve has a minimum around $V/N = 1.5$ fm^3. However, the low density part of the solid curve is unphysical, since around $V/N = 0.5$ fm^3 a phase transition occurs, and for lower densities the ground state of the system is in a chirally broken phase (dash-dotted line in Fig. (1a), labeled $\sigma \neq 0$). In this phase the values of m_q^{eff} and χ', and, consequently, σ, are no longer zero Fig. (1b)).

Performing a standard Maxwell's construction we can find the densities at which the phase transition starts and ends. They are denoted by thin arrows in Figs. (1a) and (1b). The jump in the energy per baryon number between the two phases is ~20 MeV, hence the transition is a rather weak first order phase transition. We note, however, that the "order parameters" in Fig. (1b) change abruptly from zero in the chirally restored phase to finite values in the chirally broken phase. In particular, in the vicinity of the chiral phase transition the value of σ is approximately -85 MeV, not significantly different from the vacuum value of -93 MeV, and the effective quark mass assumes values around 100 MeV. Such values are reminiscent of "constituent" quark masses, although in our case the number is about three times smaller than one third of the nucleon mass.

Note that similar values for m_q^{eff} were found in the center of baryon in chromodielectric models[2-8].

As we continue to decrease the density, the dash-dotted curve in Fig. (1a) flattens out, reaches a minimum around $V/N = 2.5$ fm^3, and then starts to increase again. However, our calculation is not reliable in this range of densities. The assumption that the matter can be described by plane-wave gas of quarks is acceptable for high densities, where we expect baryons to be melted into a quark gas. On the other hand, we know that at the nuclear saturation density $\rho_0 = 0.17$ fm^{-3}, which corresponds to $(V/N)_0 = 6$ fm^3, nuclear matter consists of well-formed nucleons, which are three-quark clusters. One can use geometrical arguments to estimate the range in which one can expect unclustered gas to be a good approximation. Using the isoscalar charge radius of the nucleon, whose experimental value is 0.72 fm, as the nucleon radius, we find that the volume occupied by the nucleon is ~ 1.6 fm^3, which is roughly a quarter of $(V/N)_0$. Thus we expect that at densities $\sim 4\ \rho_0$ the nucleons will start to overlap, and for higher densities will gradually "melt" into a quark gas. Consequently, we expect that our approximation is good for V/N less than about 1.6 fm^3. Beyond this point the clustering effects become important. Ideally, one would like to describe these effects within the model (3), this is, however, beyond the scope of this paper.

Instead, at low densities we use for comparison a traditional nuclear matter calculation. For simplicity, we have chosen the Vautherin and Brink parameterization (SI')[20] of

symmetric nuclear matter, based on the Skyrme nuclear interactions (dotted curve in Fig. (1a), labeled "Nucleonic Matter"). It is not clear up to what densities one can trust this parameterization, but we hope one can still use it up to densities $\sim 4\ \rho_0$. Also, one could use a different equation of state[21], but since we are concerned with qualitative predictions of model (3), such details would not change our general conclusions.

Looking at Fig. (1a), we note that at high densities the quark gas phase has a lower energy than the nucleonic matter, and, vice versa, at low densities the nucleonic matter is the ground state. There is a "clustering phase transition" at $V/N = 1\text{-}1.8\ fm^3$. We perform a Maxwell's construction between these two phases. The densities at which the clustering begins and ends is denoted by thick arrows in Fig. 1. We note that this phase transition should be taken with a grain of salt, since the clustered, nucleonic matter is not described within our model, but taken from elsewhere. In a consistent description, this onset of clustering may occur smoothly without a phase transition. We perform the Maxwell's construction merely to see at what densities we expect the clustering effects to become important, and find densities of the order of $3\text{-}6\ \rho_0$. This value is compatible with the number obtained earlier from geometrical estimates. Looking back at Fig. 1 (a) we can see that there is a range in densities, approximately between 6 and 12 ρ_0, for which the ground state of matter is the massive quark gas, with a broken chiral symmetry.

To convince the reader that our qualitative results do not depend on parameters chosen, Fig. 2 shows E/N calculated for two different values of G (in units of GeV), with p = 2, and also a calculation for p = 1. There is only one solid curve for the chirally restored phase, since E/N_{chiral} does not depend on G or p (cf. eqn. 9). The effect of increasing G, at a fixed p, is a decrease of the energy per baryon number in the broken phase. This can be seen comparing the dashed curve and the dot-dashed curve in Fig. 2. One can also see that a different choice of p can be "compensated" by the choice of G, as the dashed curve and the dot-dot-dashed curve in Fig. 2 are very close to each other.

The effect of changing the mass of the σ is following: As m_σ increases, in the chirally restored phase (eqn. (9)) the value of B increases, hence E/N_{chiral} goes up. In the broken phase, the increase of m_σ forces the σ field to lie closer and closer to its vacuum value $-F_\pi$, and the value of E/N also goes up.

The results of this section are of pedagogical rather than physical merit. Two-flavor matter at zero temperature and at densities of the order of a few nuclear saturation densities is not realized in nature. In the next two sections we will discuss physical cases, applicable to the neutron star physics (Sect. III) and to relativistic heavy-ion collisions (Sect. IV).

III. THREE-FLAVOR MATTER AT ZERO-TEMPERATURE

High density matter is realized in centers of neutron stars. This matter is charge neutral, and can be described in three-flavor quark models[19]. Now we apply the techniques of Sect. II to this case. For simplicity, we assume equal amounts of up, down and strange quarks, hence we neglect possible admixtures of electrons and muons, and we ignore the current mass of the strange quark. Such approximations are valid at high densities[19].

With the above simplifications, we can directly apply the formulas of Sect. II, changing the degeneracy factor γ to account for three flavors, $\gamma = 2\times3\times3$. The results are plotted in Fig. 3. In the present case, we use Pandharipande's model[22] of pure neutron matter as the traditional calculation to which we compare our results. Looking at Fig. 3, we notice that the qualitative behavior is very similar to the two-flavor case of Fig. 1. The difference is that E/N for all curves is lower for the three-flavor case, as expected from eqn. 6, and that the clustering "phase transition" occurs at higher densities, between 7 and 9 ρ_0. The massive quark phase appears at densities ~7 ρ_0, and continues up to densities ~12 ρ_0, where the chiral restoration takes place (Fig. 3).

Such high densities may be realized in centers of neutron stars, however, this depends rather sensitively on the equation of state of the nucleonic phase. For a soft equation of state the central density of the neutron star is higher than for a stiff equation of state. Therefore a soft equation of state

favors the appearance of a quark phase inside the star. In our model a neutron star would have a core of massive quarks (chirally broken phase), and, possibly, a smaller core inside, made of massless quarks (chirally restored phase). In this paper we do not quantitatively investigate this issue.

IV. FINITE-TEMPERATURE TWO-FLAVOR MATTER

In the present calculation we include only the thermal excitations of quarks, and ignore possible thermal excitations of the σ and χ' fields. This parallels the approximation of ref. 17, although a careful treatment should include thermal excitations of all degrees of freedom.

For finite temperatures, the appropriate thermodynamic potential to be minimized at fixed temperature T, volume V and chemical potential μ, is the grand potential

$$\Omega(T,V,\mu;m_q^{eff},\chi') = -TV\gamma \int d^3k/(2\pi)^3 \left\{ \ln\left[1+e^{(\mu-\nu)/T}\right] + \ln\left[1+e^{(\bar{\mu}-\bar{\nu})/T}\right] \right\} - V\left[p_\sigma + p_{\chi'}\right], \qquad (11)$$

where μ is the quark chemical potential, $\bar{\mu}$ is the antiquark chemical potential, $\nu = \sqrt{(m_q^{eff})^2 + k^2}$ is the quark single-particle energy, and $\bar{\nu}$ is the antiquark single-particle energy. Due to baryon number conservation $\bar{\mu} = -\mu$, and due to the charge conjugation symmetry $\bar{\nu} = \nu$. The quantities p_σ and $p_{\chi'}$ are the contributions to the pressure from the σ and χ' fields. In the mean-field approximation they have the form[17]

$$p_\sigma = - U(\sigma) \ , \qquad p_{\chi'} = - W(\chi) \ . \tag{12}$$

The equilibrium conditions are

$$\partial\Omega/\partial\sigma|_{T,V,\mu} = 0 \ , \qquad \partial\Omega/\partial\chi'|_{T,V,\mu} = 0 \ , \tag{13}$$

from which we find the equilibrium values of σ and χ'. Thermodynamical quantities can then be evaluated using standard expressions. In particular, we use

$$\begin{aligned} p &= -\Omega/V \ , \\ E/V &= \gamma \int d^3k/(2\pi)^3 \left\{ \nu \, n(k) + \bar{\nu} \, \bar{n}(k) \right\} \\ N/V &= \gamma \int d^3k/(2\pi)^3 \left\{ n(k) - \bar{n}(k) \right\} \end{aligned} \tag{14}$$

where the quark and antiquark distribution functions are defined through

$$n(k) = \left[1 + e^{(\nu-\mu)/T}\right]^{-1} , \quad \bar{n}(k) = \left[1 + e^{(\bar{\nu}-\bar{\mu})/T}\right]^{-1} \ . \tag{15}$$

Figure 4 shows the isotherms in the pressure - baryon density diagram. The lowest curve is for T = 0, and the interval between the isotherms is 50 MeV. The dashed lines connect the Maxwell points, between which we have coexistence of phases. Left of the dashed lines is the region of the chirally broken phase, and right of the dashed lines is the region of the chirally restored phase. Beyond the critical temperature $T_e \simeq 348$ MeV only the chirally restored phase exists.

Two phase diagrams are plotted in Fig. 5, with the regions of the chirally broken and chirally restored phases labeled $\sigma \neq 0$, and $\sigma = 0$, respectively. Figure (a) shows the temperature dependence of the baryon densities at the two Maxwell points. The baryon density at the critical point, $T_c = 348$ MeV, is zero. Figure (b) shows the temperature dependence of the pressure at the phase transition. The shaded region in Fig. (5b) is excluded from the phase space. The boundary corresponds to $N/V = 0$, and all thermodynamical states, with positive or negative baryon densities[23], lie outside the shaded region. Note that the critical baryon density is zero, thus, the regions of the two phases are disconnected, and it is not possible to pass from one phase to the other without a phase transition (as for example in the case of vapor and water).

As in the zero-temperature case, we might compare our results to some standard nuclear matter calculation, and construct the "clustering phase transition" for finit temperatures as well. We expect an appearance of the nucleonic phase in the diagrams of Figs. 4 and 5. In particular, a nucleonic region should be drawn in Fig. 5 (a) at low densities and temperatures. We have not drawn this region, since calculations of high temperature nucleonic matter are subject to large uncertainties. Traditionally, one expects that the hadronization phase transition between quark-gluon plasma and hadrons occurs at temperatures of the order of 150-300 MeV. Our results of Sect. II and the value of $T_c = 348$ MeV allow us to speculate that the nucleonic region in Fig. 5 (a) would be

contained in the chirally broken quark gas phase. In that case the chirally broken phase with massive quarks will exist at high temperatures as well. Appropriate thermodynamic conditions to generate this phase may be reached in heavy-ion collisions.

V. CONCLUSIONS

We have analyzed quark matter in a chiral chromodielectric model, investigating in detail the chiral phase transition. We have found that the quark gas phase with broken chiral symmetry may be the ground state of matter for densities of the order of a few nuclear saturation densities.

Although our calculation has been done in the framework of a specific model, and many simplifying assumptions have been used, the described behavior is of a general nature, common to models with fermions interacting with a scalar field which develops a vacuum expectation value. It was first discussed be Lee and Wick[24] in the context of nucleonic matter. The mechanism leading to the appearance of the "constituent", massive quark gas phase can be described as follows: at high densities, where the quarks are massless, there is some additional volume energy in the system. If this volume energy gets reduced when the quarks become massive, than there is a possibility of an overall decrease of energy per baryon number, and a phase transition. In our case this volume energy is interpreted as the energy necessary to break the chiral

condensate of the vacuum, and the quark masses are generated via spontaneous symmetry breaking.

Our calculation can be used to limit the range of parameters of the chromodielectric model (3). In particular, we do not want the model curves in Fig. 1 (a) to drop below the nuclear saturation energy, or to predict declustering for too low baryon densities. Such limits are useful in application of the model to baryons.

ACKNOWLEDGEMENTS

One of us (WB) thanks for the hospitality of the Institut Jozef Stefan in Ljubljana, where this research was completed.

REFERENCES

† also: Faculty of Natural Sciences and Technology, E. Kardelj Univ., P.O. BOX 64, YU-61111 Ljubljana, Yugoslavia.

1. H. B. Nielsen and A. Patkós, Nucl. Phys. **B195**, 137 (1982).
2. G. Chanfray, O. Nachtmann and H. J. Pirner, Phys. Lett. **B147**, 249 (1984).
3. W. Broniowski, T. D. Cohen and M. K. Banerjee, Phys. Lett. **B187**, 229 (1986).
4. I. Duck, Phys. Rev. **D34**, 1493 (1986).
5. M. K. Banerjee, W. Broniowski and T. D. Cohen, *"A Chiral Quark Soliton Model"*, in Chiral Solitons, ed. K.-F. Liu (World Scientific, Singapore, 1987).
6. A. Schuh and H. J. Pirner, Phys. Lett. **B173**, 19 (1986).
7. L. R. Dodd, A. G. Williams and A. W. Thomas, Phys. Rev. **D35**, 1040 (1987).
8. W. Broniowski, Fizika 19, 38 (1987), Supplement 2; *"Glueball and the Bag Formation"*, proceedings of the Workshop on Skyrmions and Anomalies, Kraków, Poland, February 20-24, 1987, ed. M. Jezabek and M. Praszałowicz, (World Scientific, Singapore, 1987).
9. G. Fai, R. J. Perry and L. Wilets, Phys. Lett. **B208**, 1 (1988).

10. J. E. Mayer and L. Sucher, Phys. Rev. D9, 3701 (1974);
K. Bitar and T. D. Lee, Phys. Rev. D13, 1694 (1977);
Ibid. D16, 1966 (1977);
F. Haselfranz and J. Kuti, Phys. Rep. 40, 75 (1978).

11. H. J. Pirner, J. Wroldsen and M. Ilgenfritz, Nucl. Phys. B294, 963 (1987).

12. M. Poljsak, Fizika 19, 47 (1987), Supplement 2.

13. S. H. Lee, T. D. Cohen and M. K. Banerjee, *"Color Dielectric Models from a Lattice Point of View"*, Univ. of Maryland preprint #89-080, November 1988.

14. C. F. Mathiot, G. Chanfray and H. J. Pirner, *"Phenomenology of Color Dielectrics in SU(3)-Color"*, submitted to Nucl. Phys. A.

15. A. Chodos, R. L. Jaffe, K. Johnson, C. B. Thorn and V. F. Weisskopf, Phys. Rev. D9, 3471 (1974).

16. M. Gel.-Mann and M. Levy, Nuovo Cimento 16, 705 (1960).

17. B. D. Serot and J. D. Walecka, in *Advances in Nuclear Physics*, ed. J. W. Negele and E. Vogt (Plenum, New York, 1986), Vol. 16, and references therein.

18. M. K. Banerjee, private communication.

19. G. Baym, *"Quark Matter"*, in Statistical Mechanics of Quarks and Hadrons, proceedings of the international symposium, Bielefield, FRG, August 24-31, 1980, ed. H. Satz (North-Holland, Amsterdam, 1981).

20. D. Vautherin and D. M. Brink, Phys. Rev. C5, 627 (1972), modified as described by D. J. Ravenhall, C. D. Benett and C. J. Pethick, Phys. Rev. Lett. 28, 978 (1972).

21. For a review see e.g. J. M. Lattimer, Ann. Rev. Nucl. Part. Sci. 31, 337 (1981).

22. V. R. Pandharipande, Nucl. Phys. A174, 641 (1971).

23. Note that due to charge conjugation symmetry, our results for thermodynamical properties are the same for matter and antimatter, i.e. are symmetric if $N/V \longrightarrow -N/V$.

24. T. D. Lee and G. C. Wick, Phys. Rev. D9, 2291 (1974).

FIGURE CAPTIONS

Fig. 1.

Zero temperature two-flavor matter, $G = 0.217$ GeV, $p = 2$.

(a) Energy per baryon number, E/N, plotted versus the volume per baryon number, V/N. The solid line ($\sigma = 0$) is the chirally restored quark-gas phase, the dash-dotted line ($\sigma \neq 0$) is the chirally broken quark-gas phase, and the dotted line is the nucleonic matter of ref. 20. The thin arrows indicate the densities where the chiral phase transition starts and ends, and the thick arrows indicate the densities at which the clustering starts and ends.

(b) Effective quark mass, m_q^{eff}, the chromodielectric field χ/G (division by G is introduced for convenience), and the negative σ field, plotted versus V/N. The line at 0 MeV in the left part of the graph shows that these quantities vanish in the chirally restored phase.

Fig. 2.

Comparison of the predictions of the model for various parameters. Solid line is the chirally restored phase, common to all values of G and p. The other lines are the chirally broken phases for various choices of parameters. The axes are as in Fig. 1 (a). Parameter G is in units of GeV.

Fig. 3.

Same as Fig. 1 (a) for the three-flavor case. Dotted line shows the neutron matter of Ref. 22.

Fig. 4.

Isotherms in the pressure - baryon density diagram for the two-flavor matter. The lowest curve is for T = 0, and the intervals between the isotherms are 50 MeV. The dashed lines connect the Maxwell points. Values of model parameters are the same as for the zero-temperature case.

Fig. 5.

Phase diagrams for the two-flavor matter. Labels $\sigma \neq 0$ and $\sigma = 0$ denote the regions of chirally broken and chirally restored phases.

(a) Baryon density vs. temperature. The solid lines are the densities at which the phase transition starts and ends.

(b) Pressure vs. temperature. The shaded region in the phase space is inaccessible (see text). The critical point is denoted by a dot. P_c is the critical pressure.

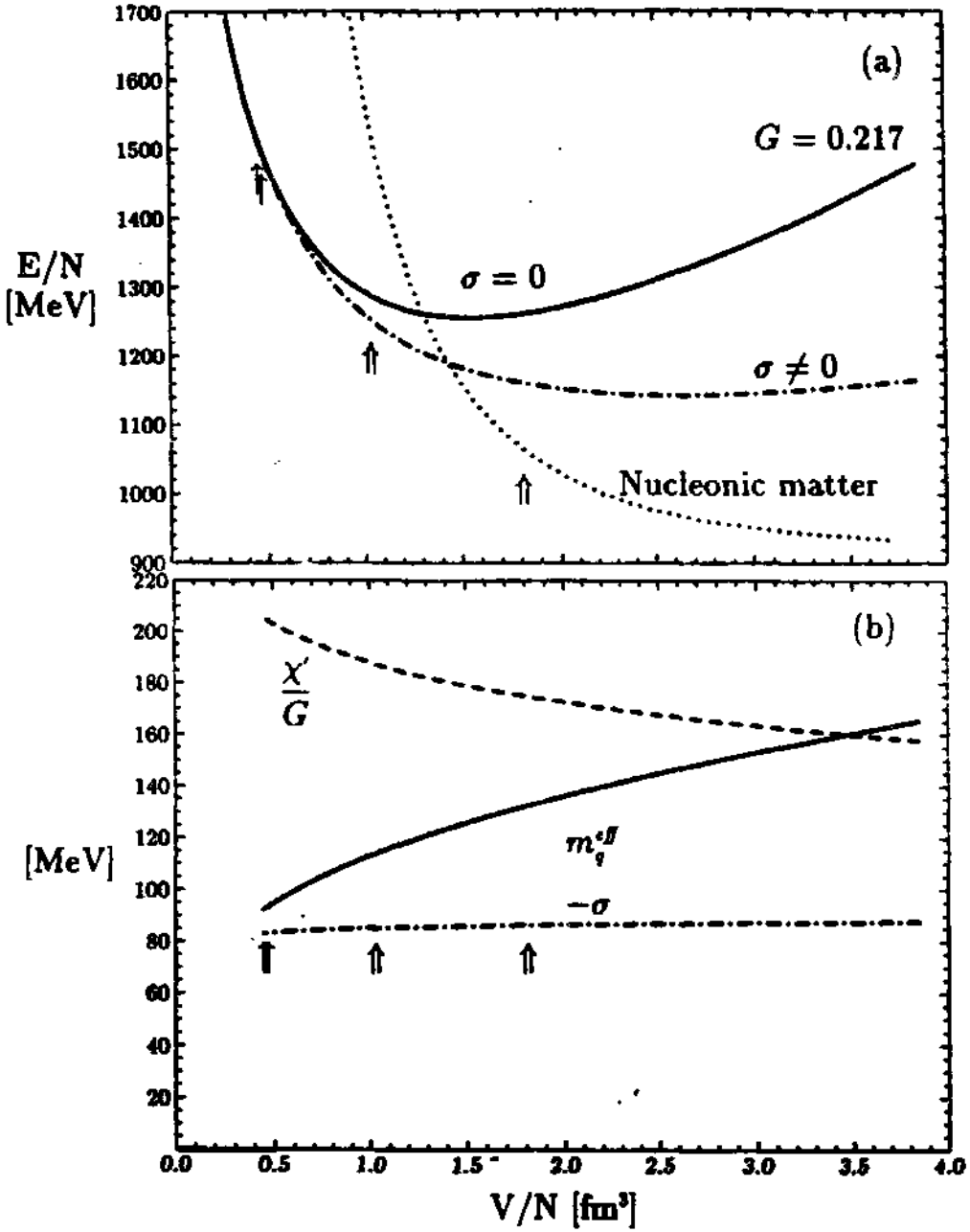
(a)
G = 0.217
σ = 0
σ ≠ 0
Nucleonic matter
E/N
[MeV]
1700
1600
1500
1400
1300
1200
1100
1000
900
(b)
χ/G
m_q^eff
−σ
[MeV]
220
200
180
160
140
120
100
80
60
40
20
0.0
0.5
1.0
1.5
2.0
2.5
3.0
3.5
4.0
V/N [fm³]

Fig. 1

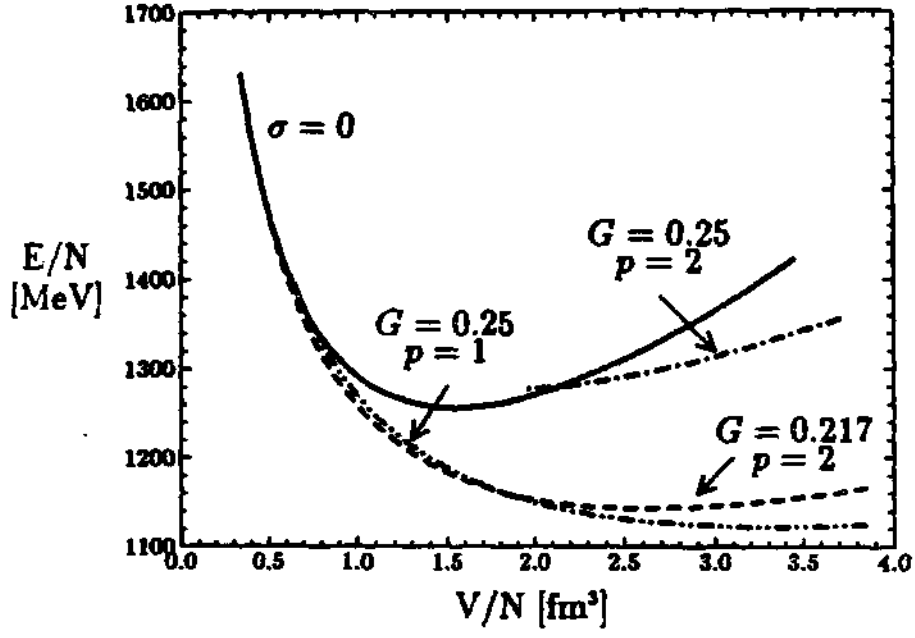
1700
1600
1500
1400
1300
1200
1100
E/N
[MeV]
$\sigma = 0$
$G = 0.25$
$p = 2$
$G = 0.25$
$p = 1$
$G = 0.217$
$p = 2$
0.0
0.5
1.0
1.5
2.0
2.5
3.0
3.5
4.0
V/N [fm³]

Fig. 2

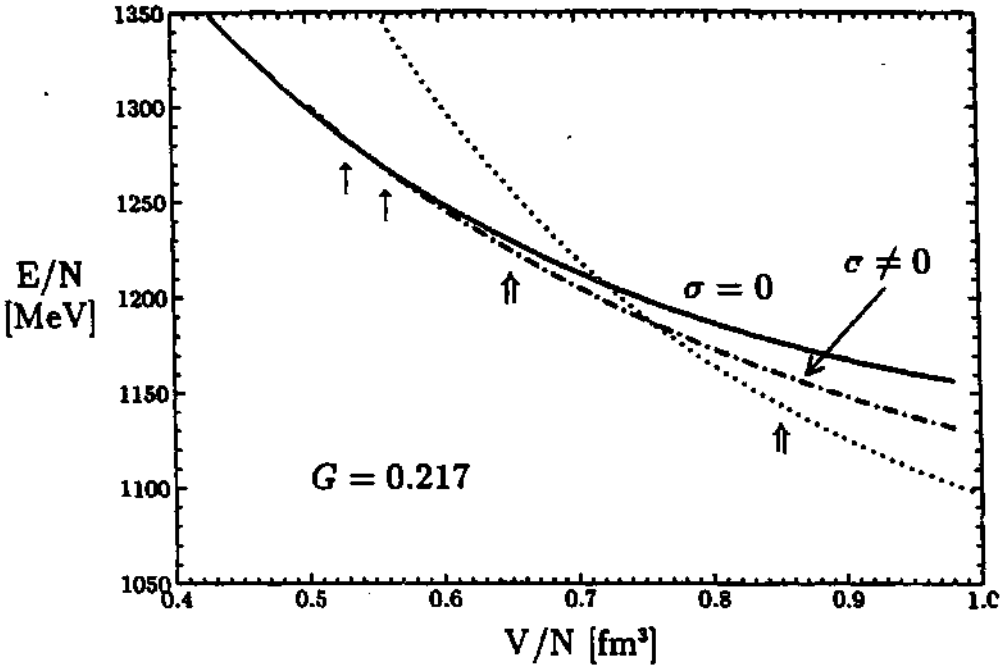
E/N
[MeV]
1350
1300
1250
1200
1150
1100
1050
0.4
0.5
0.6
0.7
0.8
0.9
1.0
V/N [fm³]
$\sigma = 0$
$\sigma \neq 0$
$G = 0.217$

Fig. 3

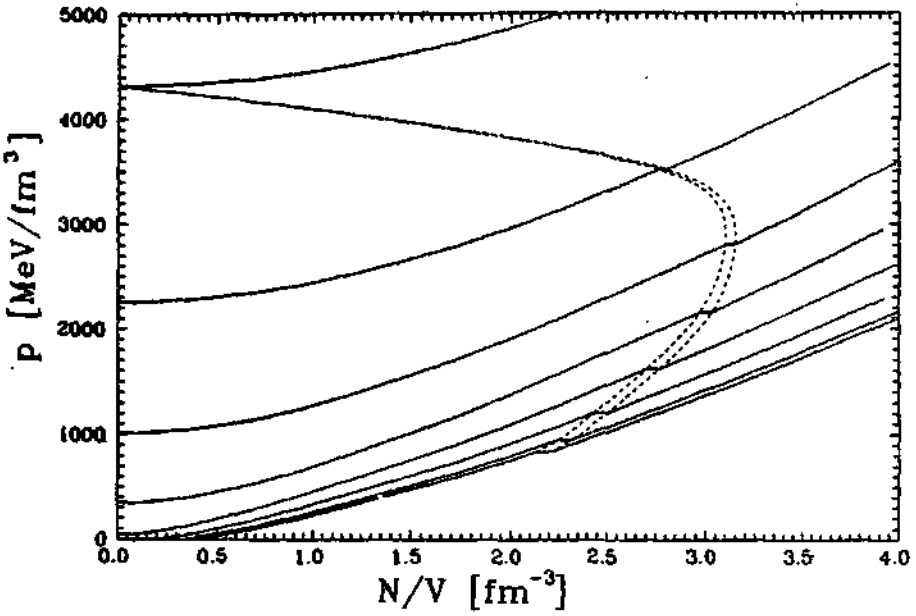
5000
4000
3000
2000
1000
0
p [MeV/fm^3]
0.0
0.5
1.0
1.5
2.0
2.5
3.0
3.5
4.0
N/V [fm^{-3}]

Fig. 4

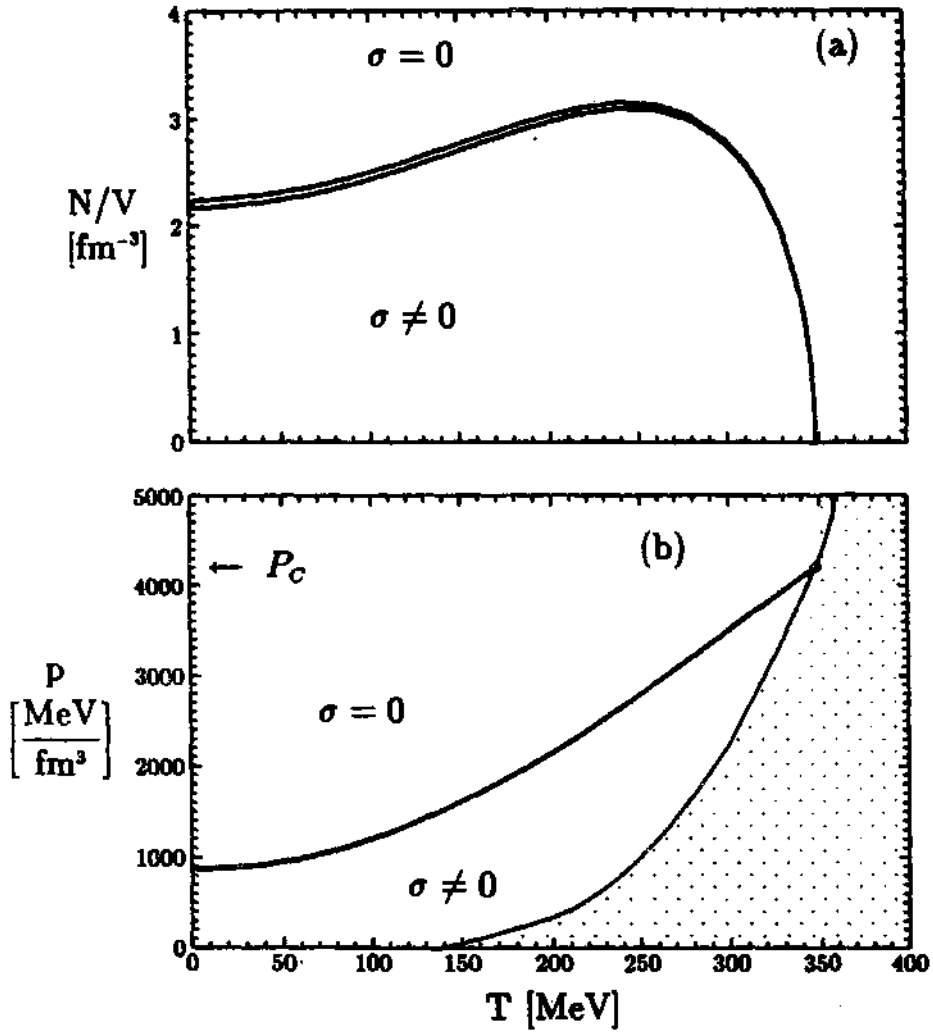

Fig. 5

IFJ Kraków, zam.57/89 100 egz.